Talanta 283 (2025) 127126

Contents lists available at ScienceDirect

Talanta

journal homepage: www.elsevier.com/locate/talanta

Recombinant bovine serum albumin domain II as bioreceptor for ochratoxin A capture

Tatiana Q. Aguiar [a,b,*,1], Tânia Leal [c,1], Diana G. Rodrigues [a], Luís Abrunhosa [a,b], Carla Oliveira [c], Lucília Domingues [a,b,**]

[a] CEB – Centre of Biological Engineering, University of Minho, 4710-057, Braga, Portugal
[b] LABBELS – Associate Laboratory, Braga/Guimarães, Portugal
[c] Universidade Católica Portuguesa, CBQF - Centro de Biotecnologia e Química Fina – Laboratório Associado, Escola Superior de Biotecnologia, Rua Diogo Botelho 1327, 4169-005, Porto, Portugal

ARTICLE INFO

Handling editor: Kin-ichi Tsunoda

Keywords:
Ochratoxin A
BSA domain II
Bioreceptor
Solid-phase extraction
Recombinant protein

ABSTRACT

Established chromatographic techniques for mycotoxin control in foodstuffs require prior sample enrichment and clean-up, typically achieved using immunoaffinity columns (IACs). Bovine serum albumin (BSA) has recently emerged as a cost-effective alternative to antibodies used in IACs. This study aimed at exploring the BSA domain II (BDII), which houses the primary binding site for ochratoxin A (OTA), as a bioreceptor for OTA capture. Recombinant BDII (rBDII) was produced in soluble form by *Escherichia coli* Origami 2(DE3), fused to a His6 (HisBDII) or thioredoxin-His6 (TrxBDII) tag, with yields up to 19 ± 4.3 mg/$L_{culture}$ in shake-flask. Fluorescence and circular dichroism (CD) spectroscopy revealed interaction of OTA with both rBDII variants, with estimated binding constants for OTA-HisBDII/TrxBDII complexes in the range of 5.7–9.3 × 10^4 M^{-1}. CD also showed an α/β structure of rBDII variants, in opposition to the predominant α-helical structure of whole BSA, and slight increase in their α-helical content upon binding to OTA. TrxBDII immobilized on Ni-NTA resin successfully captured OTA from spiked samples at the optimum pH range of 6.5–7.0, allowing OTA extraction, clean-up, and enrichment from spiked white grape juice, with up to 84 ± 7.4 % recovery.

1. Introduction

Mycotoxins are toxic secondary metabolites naturally produced by certain fungal species that are ubiquitously present in nature and contaminate various agricultural commodities. Ochratoxin A (OTA) is one of the most common and concerning food and feed contaminating mycotoxins, being linked to severe health risks to humans and animals due mainly to its nephrotoxicity and carcinogenic potential (classified as possibly carcinogenic to humans - Group 2B according to the IARC classification) [1]. With high bioaccumulation characteristics, OTA can be found in a wide variety of feed and food stuffs of plant origin, namely in cereals, grapes, coffee beans, cacao, dried spices, herbs, and their derived products, which raises additional concerns [1,2]. To mitigate the health risks associated with its consumption, maximum limits have been established in several countries and regions for various foodstuffs [3]. In the European Union, the legislation for OTA was recently extended to 30 food categories, with maximum limits generally ranging from 2 to 20 μg/kg. Exceptions include liquorice, which has limits set between 10 and 80 μg/kg, and children's foods, which have a limit of 0.5 μg/kg [4].

Several analytical methods have been successfully developed for detecting and quantifying OTA in food matrices [5]. However, conventional chromatographic-based methods remain the gold standard in most laboratories due to their sensitivity, accuracy, and precision [6,7]. High- or ultra-high-performance liquid chromatography coupled with fluorescence detection (HPLC-FD or UPLC-FD) are the most commonly used techniques for routine OTA analyses [3,8,9]. Before analysis, an effective purification and enrichment is required to release OTA from the matrix, typically followed by a clean-up step to reduce matrix interferences. Solid phase extraction (SPE) using immunosorbents immobilized on solid supports such as agarose or silica is the most commonly used method for this purpose, enabling the selective extraction, clean-up

* Corresponding author. CEB – Centre of Biological Engineering, University of Minho, 4710-057, Braga, Portugal.
** Corresponding author. CEB – Centre of Biological Engineering, University of Minho, 4710-057, Braga, Portugal.
E-mail addresses: tatiana.aguiar@ceb.uminho.pt (T.Q. Aguiar), luciliad@deb.uminho.pt (L. Domingues).
[1] Equal contributors.

https://doi.org/10.1016/j.talanta.2024.127126
Received 5 July 2024; Received in revised form 19 October 2024; Accepted 29 October 2024
Available online 30 October 2024
0039-9140/© 2024 The Authors. Published by Elsevier B.V. This is an open access article under the CC BY license (http://creativecommons.org/licenses/by/4.0/).

and enrichment of OTA in a few steps [2]. More conventional sorbents, such as reverse or normal silica, ion exchange, or mixed-mode phases can also be used, but these often require more complex and time-consuming optimizations [2,5]. Regardless of their type, SPE sorbents are usually packed in cartridges or columns, conditioned, and loaded with samples. After rinsing with an adequate washing solution to remove interferents, OTA can be eluted from the sorbent with purity and concentration levels suitable for subsequent analytical detection and quantification [2].

While very selective, reliable, and sensitive, the commonly used SPE immunoaffinity columns (IACs) based on antibodies specific to OTA have limitations, primarily their high cost and single-use nature, which restrict their broader use [5,8]. Hence, research has focused on developing alternative biorecognition molecules and materials, such as aptamers, short peptides, recombinant proteins and molecularly imprinted polymers, which have been used in mycotoxin extraction, purification, and biosensor platforms [2,3,6]. Among these, bovine and human serum albumin (BSA and HSA) have emerged as interesting alternatives to antibodies for use in OTA SPE devices due to their reasonably high affinity to this mycotoxin (10^5-10^6 M^{-1} for BSA [10,11] and 10^6-10^7 M^{-1} for HSA [11,12]), wide availability at low cost, and comparable performance to IACs [7,8].

Serum albumins are primarily obtained from animal or human plasma, but large-scale recombinant production is likely the solution to meet the increasing demand for BSA and HSA in various pharmacological, biochemical, and biotechnological applications [13]. Additionally, recombinant production allows for the engineering of serum albumins with improved stability [13], enhanced binding properties, or specific modifications that may be useful for certain applications, such as subsequent immobilization on SPE supports [14]. In this context, significant efforts have been made to develop cost-effective bioprocesses for recombinant albumin production. Microbial hosts, such as bacteria and yeast, are the most explored due to their advantages in production speed, cost and yield [13,15,16]. Among these, the best production yields have been obtained with yeast [16], as the folding of disulfide-rich multidomain albumins is challenging for bacterial hosts [13,15,17].

Structurally, serum albumins consist of three globular domains (I, II and III), each containing two subdomains (A and B), and 17 conserved disulfide bridges. The principal OTA binding site is located within domain II, specifically in Sudlow's site I (subdomain IIA), an important drug-binding site [11,12]. Studies with recombinant HSA produced by yeast revealed that the binding affinity of this domain to OTA (7.9×10^5 M^{-1}) is only one order of magnitude lower than that of the entire HSA (5.2×10^6 M^{-1}) [12].

Given that the interaction of BSA with OTA had been explored previously to develop BSA-based SPE columns for OTA determination in wine, with performances comparable to IACs [8], this work aimed at exploring the BSA domain II (BDII) as a bioreceptor for use in new OTA separation platforms. To ensure stable supply and facilitate immobilization on widely available SPE supports, this work aimed to obtain BDII recombinantly from *Escherichia coli*, fused to a His6 purification/immobilization tag (rBDII). After characterization of the interaction of rBDII with OTA, rBDII was immobilized on nickel-nitrilotriacetic acid (Ni-NTA) crosslinked agarose resin. Subsequently, the effectiveness of this rBDII-based SPE system for OTA capture was assessed.

2. Materials and methods

2.1. Cloning, recombinant production and purification of BDII fusion variants

The coding sequence for the domain II of BSA (amino acids 188–385) with codons optimized for expression in *E. coli* was purchased from NZYTech, flanked by *NcoI* and *XhoI* recognition sites at the 5′- and 3′-end, respectively. Using these restriction enzymes (New England Biolabs), BDII was cloned into the expression vector pETM10 (EMBL), in fusion with an N-terminal His6 tag (pETM10_HisBDII), and pETM20 (EMBL), in fusion with an N-terminal tag comprising the *E. coli* thioredoxin 1 (Trx), His6 and a tobacco etch virus (TEV) protease recognition site (pETM20_TrxBDII) (Table 1), as confirmed by Sanger sequencing (Eurofins Genomics). Chemically competent NZY5α *E. coli* cells (NZYTech, #MB00402) were used for plasmid construction and propagation, and *E. coli* Origami 2(DE3) (Novagen), which contains mutations that facilitate cytoplasmic disulfide bond formation, was used for protein expression.

E. coli strains were grown in LB medium (5 g/L yeast extract, 10 g/L tryptone, 10 g/L NaCl, pH 7.0) containing 50 μg/mL kanamycin (pETM10_HisBDII) or 100 μg/mL ampicillin (pETM20_TrxBDII) for plasmid selection and maintenance. 12.5 μg/mL tetracycline and 50 μg/mL streptomycin were also used to ensure the *E. coli* Origami 2(DE3) genotype. For recombinant protein production, 250 mL of medium were inoculated with 5 mL of overnight cultures and incubated at 37 °C and 200 rpm until reaching an optical density (OD_{600nm}) of ~0.5. Expression of the fusion proteins was then induced with 0.2 mM isopropyl-β-D-thiogalactopyranoside (IPTG; NZYTech, #MB02603) for ~16 h at 18 °C and 150 rpm, after which the cells were harvested by centrifugation at (10,000 rpm, 10 min, 4 °C) and stored at -20 °C until use.

For protein purification, cell pellets were defrosted and resuspended in NZY Bacterial Cell Lysis Buffer (NZYTech, #MB17802) containing 100 μg/mL lysozyme, 4 μg/mL DNaseI and 1 mM phenylmethylsulfonyl fluoride (PMSF; Sigma, #P7626) according to the manufacturer's instructions. After incubation at room temperature for 25 min in a rotator stirrer (LBX Instruments, RD80 model) set at 30 rpm, soluble cell-free extracts were collected by centrifugation (10,000 rpm, 10 min, 4 °C) and filtered through 0.22 μm PES syringe filter to obtain a cleared lysate. HisBDII and TrxBDII were purified from cleared lysates by immobilized metal ion affinity chromatography (IMAC), using a 5 mL HisTrap HP prepacked column (Cytiva, #17524802) operated with a peristaltic pump. Purification was performed according to the manufacturer's instructions, using 50 mM Tris-HCl and 150 mM NaCl (pH 8.0) as the main buffer solution, supplemented with 60 mM imidazole for equilibration and washing, and with 300 mM imidazole for elution. Samples from cleared lysates, binding, washing, and elution fractions were mixed 4:1 with 5× SDS-PAGE Sample Loading Buffer (NZYTech, #MB11701), boiled for 10 min at 95 °C and analysed by SDS-PAGE using 15 % (w/v) acrylamide gels. PageRuler Unstained Broad Range Protein Ladder (Thermo Scientific, #26630) was used as molecular weight marker, and BlueSafe (NZYTech, #MB15201) as protein stain. PD10 desalting columns (Cytiva, #17085101) were used to exchange the buffer of purified proteins according to the manufacturer's instructions. Purity was assessed by densitometry analysis of protein bands in BlueSafe stained SDS-PAGE gels using ImageJ software version 1.53, as described in Ref. [18]. The concentration of purified proteins was estimated from the absorbance at 280 nm using their corresponding theoretical molar extinction coefficients (Table 1).

2.2. Fluorescence and circular dichroism (CD) spectroscopy studies

The interaction of purified HisBDII and TrxBDII with OTA (Supelco, #34037-2 ML-R) was studied by fluorescence and CD spectroscopy in 10 mM Tris-HCl (pH 7.0). Commercial BSA (NZYTech, #MB046) was used as positive control under the same experimental conditions for comparative purposes. Fluorescence measurements were performed in a CYTATION 3 (Biotek) microplate reader using black 96-well flat bottom plates (Thermo Scientific, #611F96BK). All measurements were carried out at 25 °C after incubation of 100 μL protein (0–40 μM) with 100 μL OTA (0–10 μM) at room temperature for 15 min. Proteins and OTA were excited at an excitation wavelength (λ_{ex}) of 295 nm, with emission recorded in the 325–550 nm emission wavelength (λ_{em}) range. After a preliminary assessment of the excitation maxima for OTA-HisBDII, OTA-TrxBDII and OTA-BSA complexes, OTA was excited at λ_{ex} 380 nm, and

Table 1
Amino-acid sequence and theoretical physicochemical properties of native BSA (UniProt: P02769) and recombinant variants of its domain II produced in *E. coli* Origami 2(DE3). Molecular weight (MW), isoelectric point (pI) and molar extinction coefficient (ε) were calculated using the ProtParam tool [19], assuming all pairs of cysteine residues form cystines. In bold, italics and underlined are indicated the His6 tag, the *E. coli* thioredoxin 1 (Trx) and the tobacco etch virus (TEV) protease recognition sites, respectively.

Protein	Amino-acid sequence	MW (kDa)	pI	ε ($M^{-1}cm^{-1}$)
Mature BSA	DTHKSEIAHRFKDLGEEHFKGLVLIAFSQYLQ QCPFDEHVKLVNELTEFAKTCVADESHAGCEKSL HTLFGDELCKVASLRETYGDMADCCEKQEPERNE CFLSHKDDSPDLPKLKPDPNTLCDEFKADEKKFW GKYLYEIARRHPYFYAPELLYYANKYNGVFQECC QAEDKGACLLPKIETMREKVLASSARQRLRCASIQ KFGERALKAWSVARLSQKFPKAEFVEVTKLVTD LTKVHKECCHGDLLECADDRADLAKYICDNQDTIS SKLKECCDKPLLEKSHCIAEVEKDAIPENLPPLTAD FAEDKDVCKNYQEAKDAFLGSFLYEYSRRHPEY AVSVLLRLAKEYEATLEECCAKDDPHACYSTVF DKLKHLVDEPQNLIKQNCDQFEKLGEYGFQNAL IVRYTRKVPQVSTPTLVEVSRSLGKVGTRCCTK PESERMPCTEDYLSLILNRLCVLHEKTPVSEKV TKCCTESLVNRRPCFSALTPDETYVPKAFDEK LFTFHADICTLPDTEKQIKKQTALVELLKHKPKAT EEQLKTVMENFVAFVDKCCAADDKEACFAV EGPKLVVSTQTALA	66.4	5.60	42925
HisBDII	MK**HHHHHH**PMVLASSARQRLRCASIQKFGERA LKAWSVARLSQKFPKAEFVEVTKLVTDLTKVHKECCHG DLLECADDRADLAKYICDNQDTISSKLKECCDKPLLEKS HCIAEVEKDAIPENLPPLTADFAEDKDVCKNYQEAKD AFLGSFLYEYSRRHPEYAVSVLLRLAKEYEATLE ECCAKDDPHACYSTVFDKLKHLVDEPQN	23.8	6.05	16680
TrxBDII	*MSDKIIHLTDDSFDTDVLKADGAILVDFWAEWCG* *PCKMIAPILDEIADEYQGKLTVAKLNIDQNPGTAPK* *YGIRGIPTLLLFKNGEVAATKVGALSKGQLKEFLD* *ANLA*GSGSGHM**HHHHHH**SSGENLYFQGAMVLA SSARQRLRCASIQKFGERALKAWSVARLSQKFPKAEF VEVTKLVTDLTKVHKECCHGDLLE CADDRADLAKYICDNQDTISSKLKECCDKPLLEK SHCIAEVEKDAIPENLPPLTADFAEDKDVCKNY QEAKDAFLGSFLYEYSRRHPEYAVSVLLRLAKE YEATLEECCAKDDPHACYSTVFDKLKHLVDEPQN	37.0	5.54	32275

fluorescence emission spectra of OTA-protein complexes were obtained in the λ_{em} range of 410–550 nm. Binding constants for OTA-protein complexes were determined by non-linear fitting of OTA (0.5 μM) fluorescence emission intensity at 446–454 nm (λ_{ex} 295 nm or 380 nm) against increasing concentrations of HisBDII (0, 0.5, 1.25, 2.5, 5, 7.5, 10, 12.5, 15, 17.5, 20 μM), TrxBDII (0, 0.5, 1.25, 2.5, 5, 7.5, 10, 12.5, 15, 17.5, 20 μM) and native BSA (0, 0.05, 0.125, 0.25, 0.375, 0.5, 0.75, 1, 1.5, 2.5, 3.75 μM), using the GraphPad Prism 10.2.3 software and the equations described in Ref. [20] as detailed in Knowledgebase Article #1725 [21].

Far-UV CD spectra (190–250 nm) were recorded on a Jasco J-1500 CD spectrophotometer (Jasco) at 25 °C, using a 0.1 cm path length quartz cuvette and the following experimental parameters: bandwidth of 1 nm; data pitch of 1 nm; scanning speed of 50 nm/min, response D.I.T. of 1 s, 5 accumulations. The CD spectrum of the buffer was subtracted from each recorded spectrum. The secondary structure elements percentage was calculated from the CD spectra using the BeStSel web server [22].

2.3. OTA capturing assays

2.3.1. Construction of TrxBDII-based SPE columns

To assess rBDII as a bioreceptor for OTA capture, gravity flow SPE columns were prepared with the TrxBDII variant immobilized on His-Pur™ Ni-NTA resin (Thermo Scientific, #88222) and packed into 2 mL columns (Thermo Scientific, #89896). After the initial assessment of the maximum TrxBDII-binding capacity of the Ni-NTA resin (1.7–2.1 mg of purified TrxBDII/0.125 mL of settled resin), an excess of ~2.5 mg of purified TrxBDII in 1.5–3 mL of 50 mM Tris-HCl and 150 mM NaCl (pH 8.0) were incubated for 30 min at room temperature and 30 rpm (RD80 rotator stirrer, LBX Instruments) with 0.125 mL of settled resin previously charged with 0.1 M $NiSO_4 \cdot 6H_2O$ and equilibrated with the same Tris-HCl buffer. After incubation, the binding slurry was transferred to the packing column, followed by two washing steps to remove loosely bound TrxBDII: first with 1 mL of 50 mM Tris-HCl and 150 mM NaCl supplemented with 20 mM imidazole (pH 8.0) and then with 1 mL of the same buffer without imidazole. Samples were collected after each step for SDS-PAGE analysis and protein quantification, as described in 2.1. Columns packed with 0.125 mL of settled resin without immobilized TrxBDII were used as negative controls in OTA capturing assays.

2.3.2. Evaluation of OTA extraction from chemically defined buffered solutions

For the initial assessment of the constructed columns, chemically defined buffered solutions containing 10 μg/L OTA were prepared by diluting a 10 μg/mL OTA stock solution (Supelco, #34037-2 ML-R) in 10 mM Tris-HCl (TB) or 10 mM Na–K phosphate buffer (PB) at pH 6.0–8.0. Freshly prepared gravity flow SPE columns were equilibrated with 2 mL of the buffer under study and then loaded with 0.5 mL of 10 ng/mL OTA solution prepared in the same buffer. After collection of the flow-through, the column was washed with 3 × 0.5 mL of the same buffer, and then elution was performed with 3 × 0.5 mL of methanol containing 1 % (v/v) of acetic acid, as described in Leal et al. [8], with an incubation period of 2 min at room temperature preceding the collection of each elution fraction. The samples collected after each step of this procedure were stored separately at -20 °C and diluted 1:1 in HPLC mobile phase before OTA quantification.

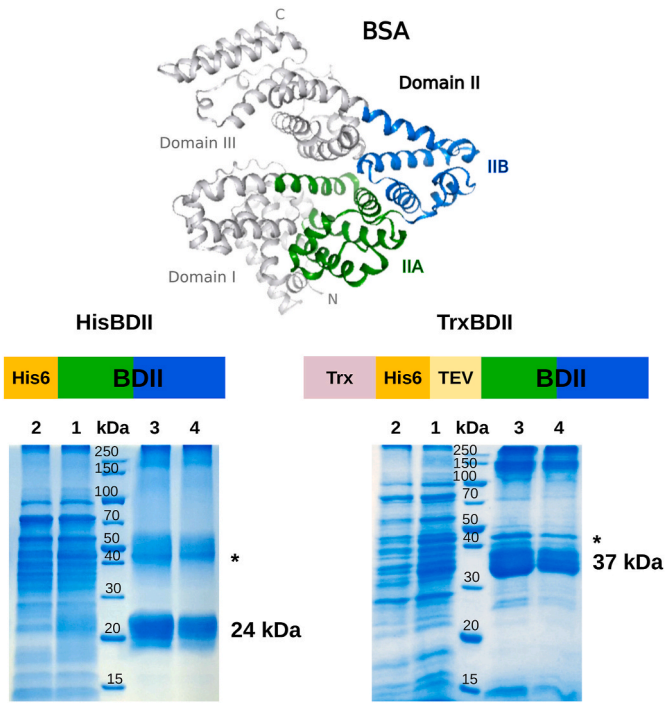

Fig. 1. BSA structure and scheme of the rBDII fusion variants produced by *E. coli* Origami 2(DE3), with BlueSafe stained SDS-PAGE gels representative of their soluble production and IMAC purification. In the scheme, the green and blue colors represent the subdomains IIA and IIB highlighted in the BSA structure with the same color. Legend of the gels: lane 1, soluble lysates from production cultures (5× diluted); lane 2, flow-through collected after passing the cleared lysates through the IMAC column (5× diluted); lanes 3 and 4, purified fractions obtained after elution; *, unknown protein from the host.

2.3.3. Evaluation of OTA extraction from spiked grape juice

To evaluate the capacity of the columns to capture, clean-up and concentrate OTA from complex food samples, bottled white grape juice randomly purchased from a local supermarket was filtered through a 0.2 μm polyamide membrane filter (Sartorius, #2500747 N) and spiked with 2 or 0.5 μg/L OTA. Then, without diluting spiked juice samples, their pH was adjusted to 6.8 by adding Tris base powder to a final molarity of ~50 mM. For these capturing assays, freshly prepared gravity flow SPE columns were equilibrated with 2 mL of 10 mM PB (pH 6.5) and then loaded with 2 mL of grape juice (pH 6.8) spiked with 2 ng/mL OTA (assay A) or 8 mL of grape juice (pH 6.8) spiked with 0.5 ng/mL OTA (assay B). After collection of the flow-through, the column was washed with 2 × 0.5 mL of 10 mM PB (pH 6.5), and elution was performed as described in 2.3.2. The samples collected after each step were stored separately at -20 °C and diluted 1:1 in HPLC mobile phase before OTA quantification.

2.4. HPLC analysis

OTA was quantified by HPLC-FD using a chromatographic system Shimadzu Nexera 40 Series coupled to an RF-20 Axs fluorescence detector (set at λ_{ex}: 333 nm, λ_{em}: 460 nm, gain: 16x-High). The column was a Synergy 2.5 μm Hydro-RP 100 A (100 × 3 mm). The eluents were filtered with a 0.2 μm membrane (Sartorius, #2500747 N) and degassed. Eluent A was acetonitrile/acetic acid (99:1, v/v) and eluent B was H_2O_{dd}/acetic acid (99:1, v/v). The isocratic separation was achieved with 45 % A and 55 % B at 30 °C and constant flow rate of 0.4 mL/min over a 10 min run. The injection volume was 10 μL. An 8-point calibration curve (10–0.04 ng/mL) was prepared by serial dilution of the primary stock (Supelco, #34037-2 ML-R) in mobile phase. OTA retention time was 8.4 min. The quantification was done by comparing the peak area of each compound with the respective calibration curve. A set of calibrants preserved at -20 °C was injected before each daily analysis. The regression delivered a linear fit: $Y = 2.22 \times 10^6$ X with an $R^2 = 0.9994$, RFRSD = 5.9 %, $n = 4$, with LOD = 0.03 ng/mL and LOQ = 0.09 ng/mL (calculated from the calibration curve by 3.3σ/s and 10σ/s, respectively).

3. Results and discussion

3.1. Recombinant production and purification of HisBDII and TrxBDII

E. coli expression strains with mutations in both the thioredoxin reductase (*trxB*) and glutathione reductase (*gor*) genes, which enhance disulfide bond formation, have been used to express soluble and functional HSA and BSA [13,15,17]. Likewise, in this work, BDII was produced by *E. coli* Origami 2(DE3) in soluble form using two IPTG-inducible expression vectors, giving rise to two different fusion proteins, HisBDII and TrxBDII (Fig. 1). Both HisBDII and TrxBDII contain an N-terminal His6 tag to facilitate purification/immobilization [18,23]. Since the *E. coli* thioredoxin 1 (Trx) is reported to improve the soluble production yield and stability of fusion partners [24,25], TrxBDII was designed with an N-terminal Trx partner, which can be removed together with the His6 tag through the TEV protease cleavage site positioned immediately before BDII (Fig. 1). Although neither rBDII fusion was easily detected in the soluble fractions of cellular lysates (Fig. 1, lane 1), bands corresponding to the predicted molecular weight of monomeric HisBDII (24 kDa) and TrxBDII (37 kDa) were visible in the elution fractions after IMAC purification (Fig. 1, lanes 3 and 4). Additionally, bands with apparent molecular weight ≥150 kDa were visible in both HisBDII and TrxBDII purified fractions. This indicates the presence of stable rBDII oligomeric forms, as already reported for purified HSA recombinantly obtained from *E. coli* [15,17]. A contaminant band of 40–50 kDa was also visible in both HisBDII and TrxBDII purified fractions, which corresponds to a native protein produced by the host that attaches tightly to the IMAC column, and which has been observed after IMAC purification of other His6-tagged proteins, namely HSA [15]. Purified HisBDII and TrxBDII could be obtained with 60–80 % purity. Despite BDII constituting only ~60 % of the molecular weight of the TrxBDII fusion protein compared to ~95 % for HisBDII, the production yields for purified rBDII with either His6 tag alone (14 ± 4.0 mg/$L_{culture}$) or the Trx-His6-TEV partner (19 ± 4.3 mg/$L_{culture}$) were identical. This indicates that the Trx partner did not improve the soluble production yield of rBDII. However, TrxBDII exhibited significantly better stability than HisBDII, as the latter displayed loss of soluble protein concentration after overnight storage at 4 °C. Untagged rBDII obtained from TrxBDII following cleavage with TEV protease also displayed low stability, precipitating after overnight storage at 4 °C. Therefore, the Trx partner apparently enhanced the stability of rBDII, as already reported for other target proteins [24,25] and further discussed in subsection 3.2. The production yields obtained here for rBDII after 16 h of IPTG-induction fall within the range of the best yields reported for recombinant HSA and BSA produced in *E. coli*, which are 10–19 mg/$L_{culture}$ [13,17]. Still, these yields are below the 65–300 mg/$L_{culture}$ reported for recombinant HSA domains (specifically domain II) produced by the yeast *Pichia pastoris* after 96–120 h of methanol-induction [26].

3.2. Interaction of OTA with recombinant HisBDII and TrxBDII

The spectral properties of OTA are known to change substantially in the presence of BSA or other albumins, and the intrinsic fluorescence of these proteins is quenched by OTA [11,27]. Thus, to examine the functionality of the produced BDII fusion variants, the ability of purified HisBDII and TrxBDII to interact with OTA was assessed by fluorescence spectroscopy.

Despite retaining the tryptophan (W) 213 residue of BSA highly sensitive to fluorescence quenching by OTA and other mycotoxins [11,

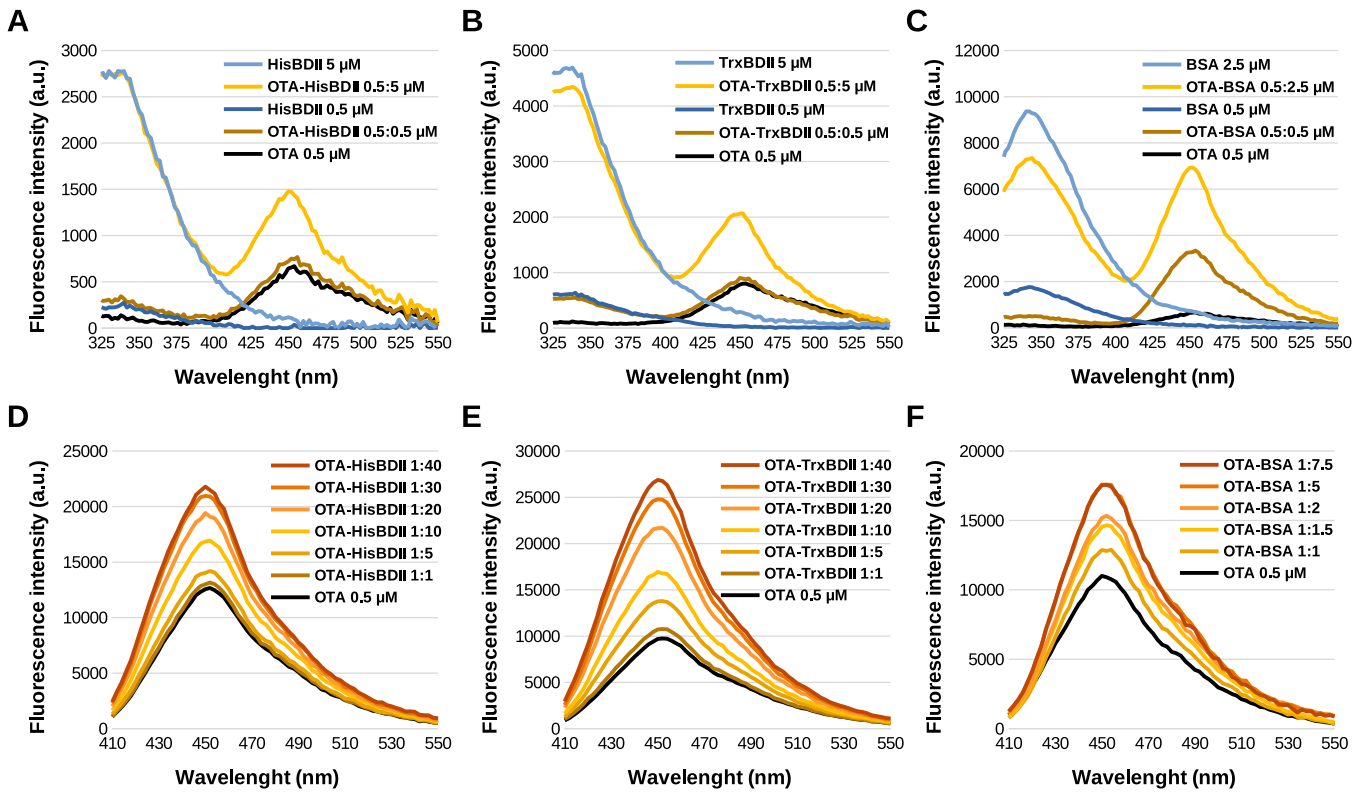

Fig. 2. Fluorescence emission spectra of HisBDII (A), TrxBDII (B), native BSA (C) and OTA (A–F), alone or in complex, at the indicated final concentration or OTA: protein ratio. All measurements were performed in 10 mM Tris-HCl (TB) at pH 7.0, using λ_{ex} 295 nm (A–C) or 380 nm (D–F). The data presented in A-B was subtracted from the residual fluorescence of the buffer and show that OTA induced a concentration-dependent decrease in the fluorescence emission signal of TrxBDII and BSA (~340 nm). The data presented in D-E was subtracted from the residual fluorescence of the buffer (for OTA) or protein at the corresponding concentration (for OTA-protein complexes) and show that HisBDII, TrxBDII and BSA induced a concentration-dependent increase in the fluorescence emission signal of OTA (~450 nm). (a.u) arbitrary unit.

28,29], the intrinsic fluorescence of HisBDII was not affected by the presence of OTA. This is evident from its identical emission at around 340 nm after excitation at 295 nm, alone (Fig. 2A, blue lines) or in the presence of OTA (Fig. 2A, yellow/brown lines). For TrxBDII, OTA induced only a slight decrease in its intrinsic fluorescence (Fig. 2B, blue lines vs yellow/brown lines), suggesting weak OTA interaction with TrxBDII. Compared to BSA (Fig. 2C), the quenching effect of OTA over TrxBDII was minimal and unsuitable for determining Stern-Volmer quenching constants. However, as observed for BSA (Fig. 2C & F), the presence of increasing concentrations of HisBDII (Fig. 2A & D) and TrxBDII (Fig. 2B & E) resulted in increasingly higher fluorescence emission intensity of OTA at around 450 nm, suggesting the formation of OTA complexes not only with TrxBDII, but also with HisBDII. This indicates that both rBDII fusion variants produced by *E. coli* are functional.

OTA displayed a fluorescence emission maximum around 450 nm both in the absence and presence of HisBDII, TrxBDII or BSA (Fig. 2), whereas its excitation maximum shifted from ~374 nm to ~381 nm upon binding to HisBDII and TrxBDII, and to ~390 nm upon binding to BSA. This red shift in the fluorescence excitation maximum of OTA in the presence of albumins has been widely reported [10,12], and the absence of the domain I has been shown to lead to the reduction of this shift [12]. Therefore, in agreement with the already reported for recombinant HSA domain II [12], HisBDII and TrxBDII did not affect the fluorescence excitation maximum of OTA as much as the entire BSA.

Based on the fitting curves presented in Supplementary Fig. S1, equilibrium constants for OTA-HisBDII, OTA-TrxBDII and OTA-BSA complexes were determined by non-linear fitting of OTA (0.5 μM) fluorescence emission intensity at 446–454 nm against increasing concentrations of HisBDII (0–20 μM), TrxBDII (0–20 μM) and native BSA (0–3.75 μM) (Table 2). These measurements were recorded using an λ_{ex} of 295 nm or 380 nm, as previously done by others [27]. The constants determined using both excitation wavelengths show good correlation and suggest the formation of stable OTA-HisBDII/TrxBDII complexes. As reported for the recombinant domain II of HSA [12], the binding constants determined here for OTA-HisBDII and OTA-TrxBDII complexes were lower (~2 orders of magnitude) than that determined for OTA-BSA. Interestingly, no substantial differences were observed between the binding constants determined for HisBDII and TrxBDII, indicating that the presence of the Trx fusion partner does not hinder the OTA-rBDII interaction. Of note, given the different origin and purity levels of the HisBDII and TrxBDII used in these assays (70–80 %) compared to the native BSA used (>98 %), these constants should be used cautiously for broader comparative purposes. Still, they provide a realistic understanding of the capturing system we are developing and studying here.

To gain further insight on the interaction of OTA with purified HisBDII and TrxBDII, CD spectroscopy studies were performed to evaluate their secondary structure and the occurrence of conformational changes induced by OTA binding. The far-UV CD spectra obtained for rBDII in fusion with the ~1 kDa His6 tag (HisBDII) or with the ~14 kDa Trx-His6 tag (TrxBDII) at the N-terminal (Fig. 3A and B) indicate structures resembling those of an α/β protein rather than those of an α-helix rich protein like BSA (Fig. 3C). Similar results were reported for the recombinant domain II of HSA, which were ascribed to the increased instability of the newly exposed long helical regions at the N and C termini of this domain [26]. While the Trx partner does not seem to alter the secondary structure of the rBDII significantly (Fig. 3D), it may enhance the stability of its N-terminal. Trx itself is a small globular

Table 2
Equilibrium constants of OTA-HisBDII, OTA-TrxBDII and OTA-BSA complexes, determined by non-linear fitting of OTA (0.5 μM) fluorescence emission intensity at 446–454 nm against increasing concentrations of HisBDII, TrxBDII and native BSA, using as λ_{ex} 295 nm or 380 nm. Data represents mean ± SE ($n = 2$).

Complex	λ_{ex} (nm)	K_D (M)	K_A (M^{-1})	logK_A	R^2
OTA-BSA	295	1.18 (±0.12) x 10^{-7}	8.47 (±0.86) x 10^{6}	6.93	0.977
	380	1.01 (±0.15) x 10^{-7}	9.91 (±1.51) x 10^{6}	7.00	0.950
OTA-HisBDII	295	1.76 (±0.09) x 10^{-5}	5.67 (±0.29) x 10^{4}	4.75	0.996
	380	1.32 (±0.11) x 10^{-5}	7.60 (±0.63) x 10^{4}	4.88	0.990
OTA-TrxBDII	295	1.08 (±0.04) x 10^{-5}	9.28 (±0.39) x 10^{4}	4.97	0.995
	380	1.38 (±0.07) x 10^{-5}	7.39 (±0.39) x 10^{4}	4.86	0.992

protein with a characteristic α/β topology [30], being composed of 31 % α-Helix, 27 % β-Sheet, 22 % Turn and 20 % Others, as determined from its PDB:2TRX resolved structure using the BeStSel web server [22]. Given its inherent properties, this fusion partner is used to improve the production yield, solubility and stability of recombinant proteins [24, 25]; and indeed, an improved stability of TrxBDII over HisBDII was observed throughout this work. On the other hand, the far-UV CD spectrum obtained for the native BSA under similar conditions (Fig. 3C) is in good agreement with published data [29], showing the two negative ellipticities of native BSA at 209 and 222 nm that are the hallmark of its rich α-helical content.

As previously reported for HSA [27], the addition of OTA to BSA induced changes in its secondary structure that led to decreased α-helicity (Fig. 3D). The presence of OTA also induced slight changes in the miscellaneous α/β structure of HisBDII and TrxBDII, but an increase in α-helical content was observed instead (Fig. 3D). The occurrence of OTA-induced conformational changes in both rBDII variants indicate that they conserve the ability of the native BSA to bind to OTA, namely in the presence of the Trx partner. However, while OTA binding induces a decrease in the α-helical content of BSA, in rBDII variants it induces a slight increase in α-helical content. These different conformational changes may be ascribed to structural and binding differences between the entire BSA, which exhibits a α-helix rich structure with at least two binding sites for OTA [12], and rBDII, whose miscellaneous α/β structure contains only one binding site for OTA.

3.3. OTA capture by TrxBDII-based SPE columns from chemically defined buffered solutions

Given the similar OTA-binding performance displayed by HisBDII and TrxBDII and the superior stability displayed by TrxBDII upon purification, namely in preliminary OTA capturing assays (data not shown), subsequent studies were performed only with TrxBDII. The suitability of TrxBDII as a bioreceptor for OTA capture was evaluated following the SPE method previously developed by our team [8], but giving a step forward in using a more cost-effective and expeditious immobilization strategy, which takes advantage of the His6 tag that was genetically fused to rBDII N-terminal for rapid site-directed immobilization on Ni-NTA resin [14]. Using this immobilization strategy, gravity flow SPE columns were prepared using 1.7–2.1 mg of purified TrxBDII immobilized on 0.125 mL of settled Ni-NTA.

In preliminary OTA capturing assays, the interaction of OTA with TrxBDII was assessed by incubating 5 ng OTA in 0.5 mL 10 mM TB pH 7.0 with immobilized TrxBDII for up to 18 h at room temperature. The percentage of unbound OTA after less than 1 min of incubation decreased to 3.2 %, and no significant changes in this percentage were seen with increasing incubation times (data not shown). These results confirmed the ability of immobilized TrxBDII to capture OTA and indicated that the interaction of OTA with this bioreceptor is almost instantaneous, not requiring long contact times. Subsequent gravity flow

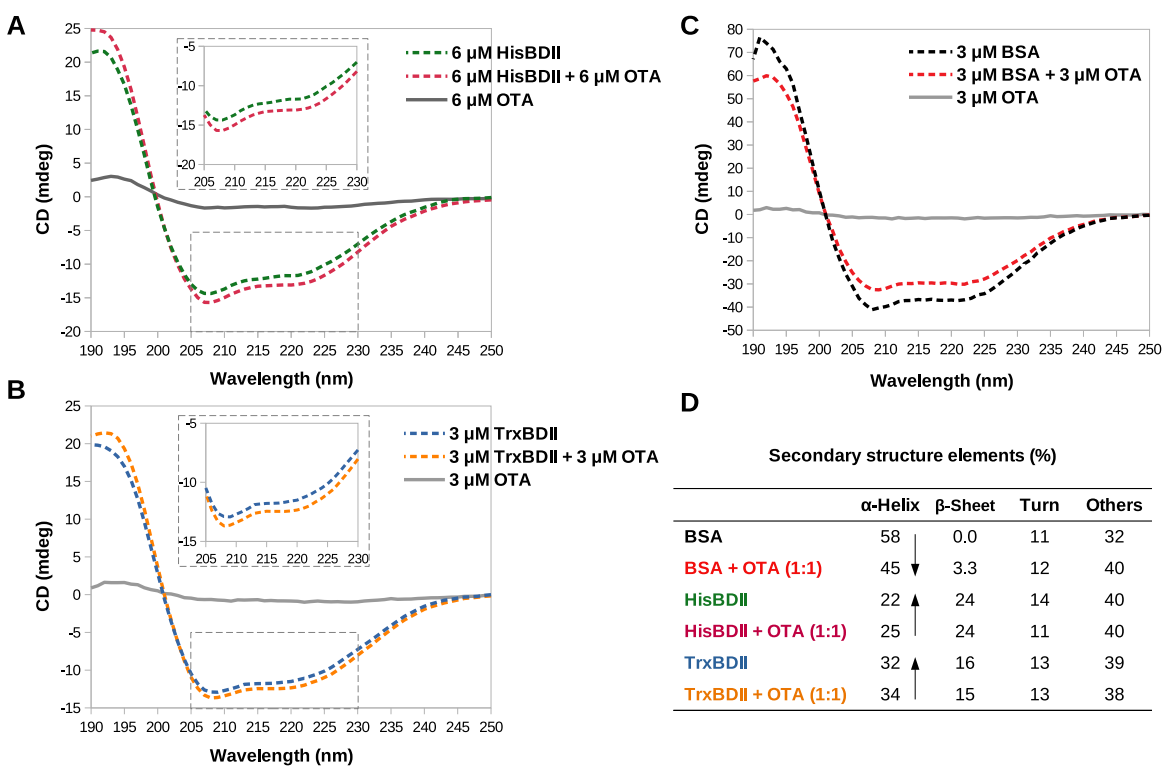

	α-Helix	β-Sheet	Turn	Others
BSA	58	0.0	11	32
BSA + OTA (1:1)	45 ↓	3.3	12	40
HisBDII	22	24	14	40
HisBDII + OTA (1:1)	25 ↑	24	11	40
TrxBDII	32	16	13	39
TrxBDII + OTA (1:1)	34 ↑	15	13	38

Fig. 3. Far-UV CD spectra of recombinant HisBDII (A), TrxBDII (B) and native BSA (C) in the absence and presence of OTA, with indication of corresponding secondary structure elements percentage calculated from the CD spectra (D). Arrows indicate a decrease (down) or increase (up) in α-helicity in the presence of OTA.

Table 3
Adsorption and desorption performance of the developed gravity flow SPE columns based on recombinant TrxBDII (~2 mg) immobilized on 0.125 mL of settled Ni-NTA resin toward OTA in chemically defined buffer solutions. OTA-capturing assays were performed at the indicated pH by loading 0.5 mL of 10 mM Tris-HCl (TB) or 10 mM Na–K phosphate buffer (PB) spiked with OTA at 10 ng/mL (equivalent to 4.7 ± 1.1 ng OTA loaded, as determined by HPLC). After three washing steps with the same buffer, OTA was eluted from the column with 1 % (v/v) acetic acid in methanol. Negative control (NC) corresponds to 0.125 mL of settled Ni-NTA resin without immobilized TrxBDII at pH 7.0. The percentage of OTA in the flow-through, wash and elution fractions was calculated from the ratio between the amount of OTA (in ng) recovered in these fractions and the amount of initially loaded OTA (which corresponds to 100 %). The indicated values (in %) represent the average (±SD) of two independent assays.

SPE step	Sample Volume	10 mM TB				10 mM PB			
		pH 6.5	pH 7.0	pH 8.0	NC	pH 6.0	pH 6.5	pH 7.0	NC
Flow-through	0.5 mL	0.0 ± 0.0	2.0 ± 0.1	10 ± 0.5	44 ± 3.2	0.0 ± 0.0	1.5 ± 0.1	0.0 ± 0.0	21 ± 1.4
Column wash	1st 0.5 mL	4.1	8.0	33	30	2.2	3.0	1.9	40
	2nd 0.5 mL	7.5	10	22	17	3.9	3.6	2.7	20
	3rd 0.5 mL	6.8	13	13	4.1	4.7	4.1	3.1	9.1
	Total	**18 ± 1.1**	**31 ± 2.1**	**68 ± 3.4**	**51 ± 0.7**	**11 ± 0.5**	**11 ± 1.6**	**8.0 ± 2.6**	**69 ± 3.7**
Elution	1st 0.5 mL	33	32	20	2.2	49	51	52	8.7
	2nd 0.5 mL	17	22	2.1	1.1	22	16	16	0.0
	3rd 0.5 mL	9.8	5.6	0.0	0.0	6.9	8.0	7.0	0.0
	Total	**60 ± 3.5**	**60 ± 3.9**	**22 ± 3.3**	**3.3 ± 1.0**	**78 ± 1.4**	**75 ± 4.5**	**75 ± 3.2**	**8.7 ± 0.4**

SPE assays preformed with 5 ng OTA in 0.5 mL 10 mM TB pH 7.0 further supported these results (Table 3). While there was also non-specific adsorption of OTA to the Ni-NTA resin (negative control), 91 % of the initially bound OTA was lost during the column washing steps (Table 3). In contrast, the column containing immobilized TrxBDII retained a greater fraction of OTA during the wash (68 %). Similar non-specific binding was reported by Leal et al. [8] using a cyanogen bromide-activated agarose resin blocked with 0.2 M glycine pH 8.0. Therefore, we decided to skip this blocking step, as it would not significantly reduce the non-specific binding of OTA. On the other hand, we observed a considerably higher loss of OTA with TrxBDII-based columns during column wash with 10 mM TB pH 7.0 (31 %) than Leal et al. [8] reported for BSA-based columns using the same buffer (0 %).

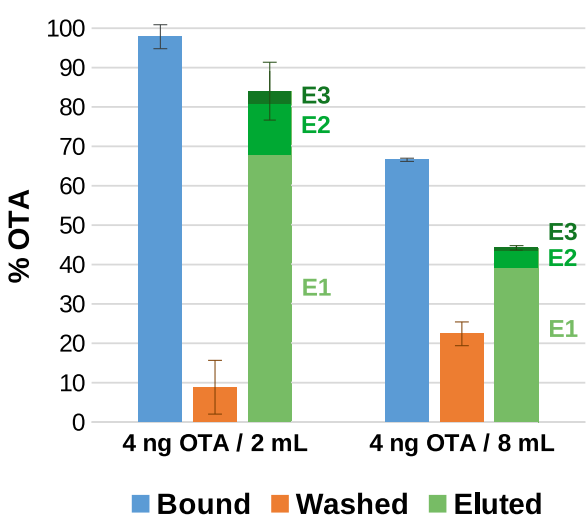

Fig. 4. Adsorption and desorption performance of the developed gravity flow SPE columns based on recombinant TrxBDII (~2 mg) immobilized on 0.125 mL of settled Ni-NTA resin toward OTA in a complex matrix. OTA-capturing assays were performed using commercial white grape juice spiked with 4 ng OTA/2 mL juice (assay A) or 4 ng OTA/8 mL juice (assay B) and with pH adjusted to 6.8 with Tris base at a final concentration of 50 mM (equivalent to 3.7 ± 0.5 ng OTA loaded, as determined by HPLC). The percentage of OTA binding to the SPE column was determined from the difference between the amount of OTA (in ng) present in the liquid matrix before (loaded fraction) and after passage through the column (unbound fraction). After two washing steps with 0.5 mL of 10 mM PB (pH 6.5), OTA was eluted from the column with 3 × 0.5 mL 1 % (v/v) acetic acid in methanol (E1-3). The percentage of OTA in the wash and elution fractions was calculated from the ratio between the amount of OTA (in ng) recovered in the wash and elution fractions and the amount of OTA present in the initially loaded matrix (which corresponds to 100 %). Bars represent the average (±SD) of three independent assays.

OTA possesses mono- and di-anionic forms, the prevalence of which is pH sensitive. At pH 7.0, both mono- and di-anionic OTA forms are present at a ratio of ~1:1 [31], but upon binding to serum albumins (namely BSA, HSA and recombinant HSA domain II), OTA suffers complete deprotonation to its di-anionic form [10,28]. However, the prevailing OTA form at pH 6.0 is the mono-anionic and at pH 8.0 is the di-anionic [31]. Thus, to study the pH influence on the interaction of OTA with immobilized TrxBDII, further capturing assays were performed using TB at pH 6.5 and 8.0. As seen in Table 3, the amount of OTA lost during the binding and washing steps was highest at pH 8.0 (78 %) and lowest at pH 6.5 (18 %), suggesting higher affinity of immobilized TrxBDII to mono-anionic OTA than to di-anionic OTA, contrary to what is reported for serum albumins (namely recombinant HSA domain II) [12]. However, the nature of the buffer used (e.g., Tris- or phosphate-based) has been reported to potentially influence protein interaction studies [23]. In this case, the existence of protonated Tris amino groups in TB at the pH range tested may have weakened the ionic interactions involved in the binding of di-anionic OTA to positively charged amino acids in the Sudlow's site I [12,28]. Thus, further assays were performed with a different buffer (10 mM PB, pH 6.0 to 7.0) to assess if improvements could be obtained in terms of OTA retention. Interestingly, using the PB buffering system, the results obtained at the different pHs tested were identical (Table 3). Compared to TB, higher retention of OTA during column wash was generally achieved with PB, which enabled superior recovery upon elution. Although higher non-specific binding of OTA to the Ni-NTA resin was observed with PB than with TB, non-specifically bound OTA was also almost entirely lost during the column wash. Considering these results, 10 mM PB (pH 6.5) was selected as the washing buffer for subsequent proof-of-concept assays. Using TB or PB (pH 6.5–7.0), the maximum binding capacity of the developed TrxBDII-based SPE columns was ~15 ng OTA (i.e, ~7.5 ng OTA per mg immobilized TrxBDII).

3.4. OTA extraction, clean-up and concentration from spiked grape juice using TrxBDII-based SPE columns

Given the interesting performance of the developed TrxBDII-based SPE columns in defined buffered solutions, the applicability of these columns to real complex samples was investigated by preparing and analysing samples of bottled white grape juice spiked with OTA at two final concentrations - 2 ng/mL (assay A) or 0.5 ng/mL (assay B) – to evaluate the effect of OTA concentration and sample volume. As seen in Fig. 4, the % of OTA bound, retained, and recovered from the column in the assay where 4 ng OTA/2 mL of juice were used (assay A) was

identical to that obtained in previous OTA-capturing assays performed with 5 ng OTA/0.5 mL PB (Table 3). Moreover, 68 % of the loaded OTA was recovered in the first elution step, with a 2.7 ± 0.2 concentration factor relative to the loaded sample, and with fewer matrix interferents (Supplementary Fig. S2A). In assay B, where 4 ng OTA/8 mL of juice were used, 56 % of the initially loaded OTA was lost during the binding and column wash steps (Fig. 4). Nevertheless, 39 % of the loaded OTA could still be recovered in the first elution step with a 6.3 ± 0.3 concentration factor (and also higher purity) relative to the loaded sample, greatly improving OTA detection (Supplementary Fig. S2B). Given that in this assay the amount of OTA loaded in the column was the same as in assay A, the lower OTA retention observed in assay B indicate that for higher juice sample volumes there may be more molecules competing with OTA binding, as several compounds found in plant-based foods and beverages can bind to the domain II of serum albumins [32].

Considering these results, the developed TrxBDII-based SPE columns performed better with lower sample volumes (assay A), allowing the recovery of up to 84 ± 7.4 % of OTA from spiked grape juice. This recovery yield falls short behind the 91–107 % OTA recovery yields obtained with immobilized BSA or HSA from spiked wine samples [7,8] or with immobilized HSA from spiked beer samples [7]. Considering the comparatively lower binding affinity of TrxBDII than native BSA (Table 2), and that the amount of immobilized TrxBDII used here (~2 mg) was lower than that previously used by Leal et al. [8] with BSA (~6 mg), additional improvements may be foreseen by increasing the amount of resin used with immobilized rBDII (which would provide more binding sites for OTA) and by further optimizing binding, washing, and elution conditions. These proof-of-concept assays thus demonstrated the suitability of immobilized TrxBDII for direct OTA extraction, clean-up and enrichment from complex white grape juice samples and the effectiveness of rBDII obtained from *E. coli* as bioreceptor for OTA capture, setting the basis for future studies.

4. Conclusion

This work demonstrated, for the first time, that His6-tagged rBDII produced and purified from *E. coli* retains the ability of native BSA to bind to OTA, albeit with lower affinity, and holds great potential as a low-cost bioreceptor for OTA capture. In solution, both rBDII versions (HisBDII and TrxBDII) undergo slight conformational changes in their secondary structure upon binding to OTA. After rapid site-directed immobilization on Ni-NTA resin through the His6 tag fused to the BDII N-terminal, rBDII maintained its OTA-binding capacity. Utilizing this straightforward and cost-effective immobilization strategy, we developed new gravity flow SPE columns based on immobilized TrxBDII, enabling direct extraction, clean-up, and enrichment of OTA from spiked white grape juice samples, with up to 84 ± 7.4 % recovery. While we performed the purification and immobilization of His6-tagged rBDII in two steps for better control over the amount of immobilized protein, future studies may consider combining these steps into a single process to simplify and speed up the production of rBDII-based SPE columns [14]. This streamlined approach has the potential to further enhance the practical application and commercial viability of rBDII-based systems for OTA detection and analysis.

CRediT authorship contribution statement

Tatiana Q. Aguiar: Writing – review & editing, Writing – original draft, Methodology, Investigation, Formal analysis, Conceptualization. **Tânia Leal:** Writing – original draft, Methodology, Investigation, Formal analysis. **Diana G. Rodrigues:** Methodology, Investigation, Formal analysis. **Luís Abrunhosa:** Writing – review & editing, Supervision, Methodology, Funding acquisition, Formal analysis, Conceptualization. **Carla Oliveira:** Writing – review & editing, Supervision, Methodology, Formal analysis, Conceptualization. **Lucília Domingues:** Writing – review & editing, Supervision, Funding acquisition, Conceptualization.

Declaration of competing interest

The authors declare that they have no known competing financial interests or personal relationships that could have appeared to influence the work reported in this paper.

Acknowledgements

This study was supported by the Portuguese Foundation for Science and Technology (FCT) under the scope of the strategic funding of UIDB/04469/2020 unit (https://doi.org/10.54499/UIDB/04469/2020) and Project MycoProAffinity (https://doi.org/10.54499/2022.03438.PTDC). Luís Abrunhosa acknowledges FCT for the assistant research contract CEECIND/00728/2017. The authors would also like to acknowledge Heiðar Aðalsteinsson, Lavínia Pinto and Rui M. Rodrigues for their assistance in CD spectroscopy analyses.

Appendix A. Supplementary data

Supplementary data to this article can be found online at https://doi.org/10.1016/j.talanta.2024.127126.

Data availability

Data will be made available on request.

References

[1] W.-C. Liu, K. Pushparaj, A. Meyyazhagan, V.A. Arumugam, M. Pappuswamy, H. K. Bhotla, R. Baskaran, U. Issara, B. Balasubramanian, A. Mousavi Khaneghah, Ochratoxin A as an alarming health threat for livestock and human: a review on molecular interactions, mechanism of toxicity, detection, detoxification, and dietary prophylaxis, Toxicon 213 (2022) 59–75, https://doi.org/10.1016/j.toxicon.2022.04.012.

[2] V. Pichon, A. Combès, Selective tools for the solid-phase extraction of Ochratoxin A from various complex samples: immunosorbents, oligosorbents, and molecularly imprinted polymers, Anal. Bioanal. Chem. 408 (2016) 6983–6999, https://doi.org/10.1007/s00216-016-9886-0.

[3] Y. Wang, C. Zhang, J. Wang, D. Knopp, Recent progress in rapid determination of mycotoxins based on emerging biorecognition molecules: a review, Toxins 14 (2022) 73, https://doi.org/10.3390/toxins14020073.

[4] European Commission, Commission Regulation (EC) 2023/915 of 25 April 2023 on maximum levels for certain contaminants in food and repealing Regulation (EC) No 1881/2006, Off. J. Eur. Union L119 (2023) 103–157.

[5] E. Janik, M. Niemcewicz, M. Podogrocki, M. Ceremuga, L. Gorniak, M. Stela, M. Bijak, The existing methods and novel approaches in mycotoxins' detection, Molecules 26 (2021) 3981, https://doi.org/10.3390/molecules26133981.

[6] Y. Alhamoud, D. Yang, S.S. Fiati Kenston, G. Liu, L. Liu, H. Zhou, F. Ahmed, J. Zhao, Advances in biosensors for the detection of ochratoxin A: bio-receptors, nanomaterials, and their applications, Biosens. Bioelectron. 141 (2019) 111418, https://doi.org/10.1016/j.bios.2019.111418.

[7] J. Ye, H. Bao, M. Zheng, H. Liu, J. Chen, S. Wang, H. Ma, Y. Zhang, Development of a novel magnetic-bead-based automated strategy for efficient and low-cost sample preparation for ochratoxin A detection using mycotoxin–albumin interaction, Toxins 15 (2023) 270, https://doi.org/10.3390/toxins15040270.

[8] T. Leal, L. Abrunhosa, L. Domingues, A. Venâncio, C. Oliveira, BSA-based sample clean-up columns for ochratoxin A determination in wine: method development and validation, Food Chem. 300 (2019) 125204, https://doi.org/10.1016/j.foodchem.2019.125204.

[9] L.J.G. Silva, A.C. Teixeira, A.M.P.T. Pereira, A. Pena, C.M. Lino, Ochratoxin A in beers marketed in Portugal: occurrence and human risk assessment, Toxins 12 (2020) 249, https://doi.org/10.3390/toxins12040249.

[10] F.S. Chu, Interaction of ochratoxin A with bovine serum albumin, Arch. Biochem. Biophys. 147 (1971) 359–366, https://doi.org/10.1016/0003-9861(71)90391-2.

[11] M. Poór, Y. Li, G. Matisz, L. Kiss, S. Kunsági-Máté, T. Kőszegi, Quantitation of species differences in albumin–ligand interactions for bovine, human and rat serum albumins using fluorescence spectroscopy: a test case with some Sudlow's site I ligands, J. Lumin. 145 (2014) 767–773, https://doi.org/10.1016/j.jlumin.2013.08.059.

[12] Y.V. Il'ichev, J.L. Perry, F. Rüker, M. Dockal, J.D. Simon, Interaction of ochratoxin A with human serum albumin. Binding sites localized by competitive interactions with the native protein and its recombinant fragments, Chem. Biol. Interact. 141 (2002) 275–293, https://doi.org/10.1016/S0009-2797(02)00078-9.

[13] O. Khersonsky, M. Goldsmith, I. Zaretsky, S. Hamer-Rogotner, O. Dym, T. Unger, M. Yona, Y. Fridmann-Sirkis, S.J. Fleishman, Stable mammalian serum albumins

designed for bacterial expression, J. Mol. Biol. 435 (2023) 168191, https://doi.org/10.1016/j.jmb.2023.168191.

[14] A.I. Freitas, L. Domingues, T.Q. Aguiar, Tag-mediated single-step purification and immobilization of recombinant proteins toward protein-engineered advanced materials, J. Adv. Res. 36 (2022) 249–264, https://doi.org/10.1016/j.jare.2021.06.010.

[15] A. Sharma, T.K. Chaudhuri, Revisiting *Escherichia coli* as microbial factory for enhanced production of human serum albumin, Microb. Cell Factories 16 (2017) 173, https://doi.org/10.1186/s12934-017-0784-8.

[16] W. Zhu, R. Xu, G. Gong, L. Xu, Y. Hu, L. Xie, Medium optimization for high yield production of human serum albumin in *Pichia pastoris* and its efficient purification, Protein Expr. Purif. 181 (2021) 105831, https://doi.org/10.1016/j.pep.2021.105831.

[17] M.T. Nguyen, Y. Heo, B.H. Do, S. Baek, C.J. Kim, Y.J. Jang, W. Lee, H. Choe, Bacterial overexpression and purification of soluble recombinant human serum albumin using maltose-binding protein and protein disulphide isomerase, Protein Expr. Purif. 167 (2020) 105530, https://doi.org/10.1016/j.pep.2019.105530.

[18] T.Q. Aguiar, L. Domingues, Recombinant protein purification and immobilization strategies based on peptides with dual affinity to iron oxide and silica, Biotechnol. J. 18 (2023) 2300152, https://doi.org/10.1002/biot.202300152.

[19] E. Gasteiger, C. Hoogland, A. Gattiker, S. Duvaud, M.R. Wilkins, R.D. Appel, A. Bairoch, Protein Identification and analysis tools on the ExPASy server, in: J. M. Walker (Ed.), Proteomics Protoc. Handb., Humana Press, Totowa, NJ, 2005, pp. 571–607, https://doi.org/10.1385/1-59259-890-0:571.

[20] H.J. Motulsky, R.R. Neubig, Analyzing binding data, Curr. Protoc. Neurosci. 52 (7.5.1–7.5.65) (2010), https://doi.org/10.1002/0471142301.ns0705s52.

[21] GraphPad, Fitting binding of fluorescent ligands, Knowledgebase Article #1725, https://www.graphpad.com/support/faq/fitting-binding-of-fluorescent-ligands/, 2011. (Accessed 19 January 2024).

[22] A. Micsonai, É. Moussong, F. Wien, E. Boros, H. Vadászi, N. Murvai, Y.-H. Lee, T. Molnár, M. Réfrégiers, Y. Goto, Á. Tantos, J. Kardos, BeStSel: webserver for secondary structure and fold prediction for protein CD spectroscopy, Nucleic Acids Res. 50 (2022) W90–W98, https://doi.org/10.1093/nar/gkac345.

[23] A.I. Freitas, L. Domingues, T.Q. Aguiar, Bare silica as an alternative matrix for affinity purification/immobilization of His-tagged proteins, Sep. Purif. Technol. 286 (2022) 120448, https://doi.org/10.1016/j.seppur.2022.120448.

[24] S. Costa, A. Almeida, A. Castro, L. Domingues, Fusion tags for protein solubility, purification and immunogenicity in *Escherichia coli*: the novel Fh8 system, Front. Microbiol. 5 (2014) 63, https://doi.org/10.3389/fmicb.2014.00063.

[25] M. Schenkel, A. Treff, C.M. Deber, G. Krainer, M. Schlierf, Heat treatment of thioredoxin fusions increases the purity of α-helical transmembrane protein constructs, Protein Sci. 30 (2021) 1974–1982, https://doi.org/10.1002/pro.4150.

[26] M. Dockal, D.C. Carter, F. Rüker, The three recombinant domains of human serum albumin, J. Biol. Chem. 274 (1999) 29303–29310, https://doi.org/10.1074/jbc.274.41.29303.

[27] F. Sueck, M. Poór, Z. Faisal, C.G.W. Gertzen, B. Cramer, B. Lemli, S. Kunsági-Máté, H. Gohlke, H.-U. Humpf, Interaction of ochratoxin A and its thermal degradation product 2′R-ochratoxin a with human serum albumin, Toxins 10 (2018) 256, https://doi.org/10.3390/toxins10070256.

[28] Y.V. Il'ichev, J.L. Perry, J.D. Simon, Interaction of ochratoxin A with human serum albumin. Preferential binding of the dianion and pH effects, J. Phys. Chem. B 106 (2002) 452–459, https://doi.org/10.1021/jp012314u.

[29] M.A. Qureshi, S. Javed, Aflatoxin B_1 induced structural and conformational changes in bovine serum albumin: a multispectroscopic and circular dichroism-based study, ACS Omega 6 (2021) 18054–18064, https://doi.org/10.1021/acsomega.1c01799.

[30] D.S. Vazquez, I.E. Sánchez, A. Garrote, M.P. Sica, J. Santos, The *E. coli* thioredoxin folding mechanism: the key role of the C-terminal helix, Biochim. Biophys. Acta BBA - Proteins Proteomics 1854 (2015) 127–137, https://doi.org/10.1016/j.bbapap.2014.11.004.

[31] I. Cagnasso, G. Tonachini, S. Berto, A. Giacomino, L. Mandrile, A. Maranzana, F. Durbiano, Comprehensive study on the degradation of ochratoxin A in water by spectroscopic techniques and DFT calculations, RSC Adv. 9 (2019) 19844–19854, https://doi.org/10.1039/C9RA02086A.

[32] A. López-Yerena, M. Perez, A. Vallverdú-Queralt, E. Escribano-Ferrer, Insights into the binding of dietary phenolic compounds to human serum albumin and food-drug interactions, Pharmaceutics 12 (2020) 1123, https://doi.org/10.3390/pharmaceutics12111123.